EMITTANCE CHARACTERISATION OF HIGH BRIGHTNESS BEAMS IN THE CERN PS

G. Sterbini, J.-F. Comblin, V. Forte, A. Guerrero, E. Piselli, CERN, CH-1211 Geneva 23

Abstract

Measurements in the CERN Proton Synchrotron showed that achieving the required accuracy for the emittance characterisation of high brightness beams is challenging. Some of the present limits can be related to systematic errors in the wire scanner calibration or, for the horizontal emittance determination, in the assumptions adopted while deconvoluting the contribution of the longitudinal plane from the measured transverse profile. We present in this paper the results of a beam-based test of the wire scanner calibration and of a general numerical deconvolution algorithm to compute the betatronic profile starting from the measured ones. In addition to the bunch train average emittance, a bunch-by-bunch transverse emittance measurement would increase the potential to understand, optimise and monitor the beam performance. In 2015 the first PS bunch-by-bunch measurement chain was setup. The results are reported and discussed.

INTRODUCTION

The LHC Injector Upgrade (LIU) aims to increase by about a factor two the brightness of the beams provided by the Injector Complex to the LHC [1]. To achieve this goal the transverse emittance blow-up (ϵ_n) budget in the CERN Proton Synchrotron (PS) is strict (5%) [2]. This constraint automatically sets upper limits to the precision and accuracy of the measurement of the ϵ_n. In the past years, measurement in the CERN Proton Synchrotron (PS) showed that these limits are challenging to meet for low emittance beams [3]. This is particularly true for the horizontal plane, where the measured transverse beam profile is the convolution of the betatronic one and the one due to the dispersion and the beam energy distribution.

Presently, the evolution of the ϵ_n in the PS is monitored and optimised by using 3 horizontal and 2 vertical wire scanners (WS) [4] [5]. The machine is also equipped with 3 SEM grid devices (each device has a horizontal and vertical grid) but can be presently used only for measuring the beam's first turn [6]. In the PS ring, there are also 5 scintillating screens installed in injection/extraction channel of the septa [7] used mostly for beam steering. In order to improve the diagnostic tools for the ϵ_n characterization, a new WS mechanical design will be adopted [8] and a beam rest gas ionization monitor prototype (BGI) is going to be installed in the machine in 2016 [9].

THE BEAM-BASED WS CALIBRATION

In contrast to SEM grids, the screens or the BGI, the WS is moving during the measurement (flying wires). For a correct reconstruction of the beam profile, the accuracy of the knowledge of the wire position is critical. This is obtained by a calibration function, f (measured in a calibration bench), that relates the signal, m, from a potentiometer installed on the WS motor with the wire position projected on the plane perpendicular to the beam direction, x ($x = f(m)$). It is important to note that adding to f an constant error with respect to m will affect the reconstructed position of the beam profile (offset error) but will not affect the accuracy of ϵ_n. On the other hand an error in $\frac{df}{dm}$ can directly impact on the beam reconstructed profile accuracy (therefore on ϵ_n and/or beam tail characterisation). During the 2015 run, the calibration of two horizontal WS was compared with a beam-based WS calibration. This is usually done using local orbit bumps. In our case, we used the radial steering capability of the PS beam control: this allows a large horizontal excursion of the beam even at top energy and use all 43 pick-ups (PUs) for a better conditioning of the problem. From the performed measurement, we observed that the dispersion of the machine, D_x, is linear within the explored off-momentum, $\frac{\Delta p}{p}$. This can be concluded by inspection of the singular values (SVs) of the acquired orbit matrix (the horizontal dispersion, D_x, is linear if there is one dominating singular value, Fig. 1) or by a trivial correlation between all the different pick-ups (see Fig 1 lower plot). The left and right singular vectors (respectively u_1 and v_1) corresponding to the dominant SV will be respectively proportional to the dispersion in the 43 PUs and the $\frac{\Delta p}{p}$ of the different measurements. Comparing the horizontal and vertical planes SVs (Fig. 1) one can observe that the spuri-

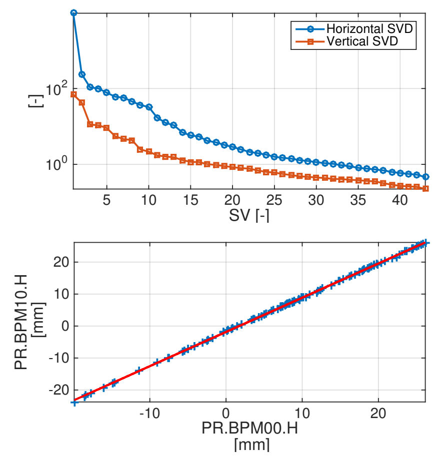

Figure 1: Singular values of the dispersive orbits in the horizontal and vertical planes (top). An example of correlation between two PUs (bottom). From the two plots we can conclude that the D_x within the $\frac{\Delta p}{p}$ region explored during the radial scan.

ISBN 978-3-95450-147-2

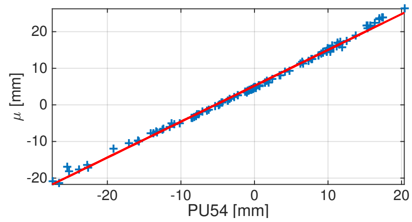

Figure 2: Correlation between the position read by the WS54 and the nearby PU.

ous dispersion in the vertical plane, D_y, is $\approx$ 100 smaller than the horizontal one. D_y can be due to spurious vertical dipolar components, PU tilt errors and coupling between the transverse planes. We observed a good correlation between the v_1 obtained from the horizontal and vertical SV analysis confirming its overall consistency. During the radial steering scan, we performed WS measurement using both WSs in the straight section 54 (WS54) and 68 (WS68) with 10 and 15 m/s speed respectively. The measurement was done at top energy (26 GeV) with a LHC type single bunch (pencil beam) using the "IN" scan movement. We used the WS as PU by defining the position of the beam at the WS location as the center, μ, of the 5-parameter Gaussian fit [3]. From the above consideration we expect to have a linear relation between the v_1 and μ. In Fig. 2, we show the results of the measurement for WS54. This measurement puts in evidence minor errors in the linearity of the μ. It is important to note that this check is based only on the linearity of the dispersion and is not affected by possible PU calibration errors. On the other hand to make a complete WS beam-based calibration we need to measure or compute the dispersion at the WS. In the PS, all the WS have a nearby PU ($\approx$ 50 cm apart). From a linear optics model of the machine one can verify that the dispersion difference from the PU and the WS is $< 1‰$. Therefore one can derive the dispersion at the WS using nearby PU and assuming that the calibration errors of the PU itself is negligible. This hypothesis was checked using the linear model of the machine: in Fig. 3 we show the computed D_x (solid line) and the one obtained by u_1 after having applied a scaling factor. It is possible to note that only a fraction of the PU (black circles) behave as expected. Further investigations are therefore needed to verify the calibrations of the other PUs (red crosses).

DECONVOLUTION ALGORITHM

The WS transverse beam distribution, ρ_{WS}, is the convolution of the dispersive distribution, ρ_{D_x}, and the betatronic one, ρ_{β_x}. The ρ_{β_x} is the relevant one for our purpose since related to the transverse emittance. In the vertical plane, we neglect the contribution of the dispersion. In the horizontal plane ρ_{D_x} can be derived from the energy distribution $\rho_{\frac{\Delta p}{p}}$ obtained, under the assumptions of the matched longitudinal phase space, by the Abel transform of the measurable longitudinal profile, $\rho_{\Delta t}$ [10, 11]. To obtain ρ_{β_x} from ρ_{WS} and ρ_{D_x} we need to solve a convolution equation. The present ap-

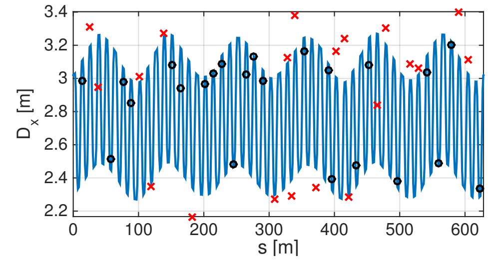

Figure 3: Comparison between measured (markers) and simulated dispersion (solid line). The red markers represent values in disagreement with the model.

proach used to compute ρ_{β_x} is to assume that ρ_{WS} and ρ_{D_x} (and therefore ρ_{β_x}) are normal distributions. This approximation introduces systematic errors in particular for low transverse emittance and large longitudinal emittance beams. Recently it was proposed to use a deconvolution algorithm assuming that only ρ_{β_x} is a normal distribution [12, 13]. In the following we discuss a deconvolution algorithm to relax also this hypothesis. This algorithm can be used in complement and for comparison with the previous two to investigate the tail distribution of ρ_{β_x}. The stability of the presented algorithm is limited and particular attention has to be devoted in minimizing the noise of the measurement (i.e., by averaging). For the deconvolution, we used the approach described in [14]. The numerical convolution $\rho_{WS} = \rho_{D_x} \otimes \rho_{\beta_x}$ can be rewritten as a matrix multiplication, where one of the inputs, ρ_{D_x}, is converted into a Toeplitz matrix (i.e., a diagonal constant matrix), H ($\rho_{WS} = H\ \rho_{\beta_x}$). Solving the problem with a least-square approach and using a regularization on the second order derivative of ρ_{β_x}, one has

$$\rho_{\beta_x} = (H^T H + \lambda D^T D)^{-1} H^T \rho_{WS} \tag{1}$$

where λ is the regularization parameter and D is the second difference matrix

$$D = \begin{bmatrix} 1 & -2 & 1 & & & \\ & & \ddots & \ddots & \ddots & \\ & & & 1 & -2 & 1 \end{bmatrix}. \tag{2}$$

An example of the result of the algorithm is shown in Fig. 4. For this example we used an heavy-tail ρ_{β_x}. If the noise level is negligible the ρ_{β_x} can be reconstructed with no error. If we apply the same algorithm considering noise in the ρ_{WS} and ρ_{D_x} distributions, the precision on the reconstructed profile is limited. In any case, the high-frequency noise can be reduce with a Fourier filter before applying the Eq. 1.

THE BUNCH-TO-BUNCH EMITTANCE MEASUREMENT

During the 2015, the first PS bunch-by-bunch measurement chain was setup. This kind of measurement can reveal differences in the brightness in the bunches injected from the PS Booster (PSB) and allow to investigate emittance blow-up along the bunch train during the PS cycle. Most of

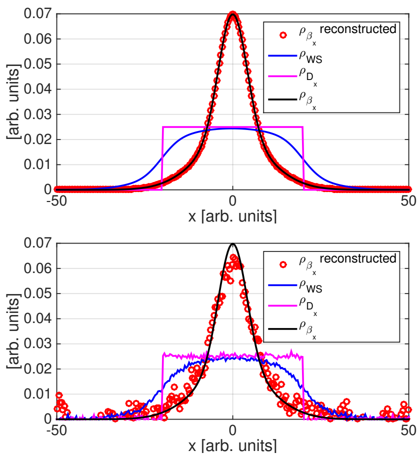

Figure 4: Deconvolution without noise in the measured signal, λ = 0 (above). Simulating the effect of noise, λ = 0.003 (below).

Figure 5: An example of signal obtained from the WS PM numerical gating in h=84 (less than three turn are shown).

the hardware for the bunch-by-bunch measurement is shared with the turn-by-turn measurement but the high bandwidth cables connecting the two WS photomultipliers (PM) with the front-end electronics and the acquisition card to gate the PM signal with $f_{gate} = 84 f_{rev}$. The gating electronics is not yet fully commissioned. For our measurement, we acquired the PM signal and the beam f_{rev} signal directly on an oscilloscope. The oscilloscope was triggered by the WS trigger and the signal acquired at maximum sampling (1 GS/s), typically, in a 5 ms time window (compatible the the WS time-of-flight in the beam). The gating was numerically done during the post-processing combining the two signals. An example of the gating of one of the two signals is shown in Fig. 5. The measurements were done for different beams (LHC and nToF type), different harmonics (h=7, 8, 21, 84) and energies (injection and extraction energy). One of the main concerns of the bunch-by-bunch measurement is the cross-talk of adjacent bunches. To explore this limit, we introduced fast bunch-by-bunch emittance variation along the batch by injecting 6 bunches with different emittances (this can be done by varying the bunch intensity in the PSB). Each of the 6 injected bunches are split longitudinally in 12 bunches (from h=7 to h=84) during the PS LHC cycle. Using bunch-by-bunch WS measurement at top energy we expect to see beam sigmas grouped in 7 clusters according to the original bunch emittance. The results are shown in Fig. 6.

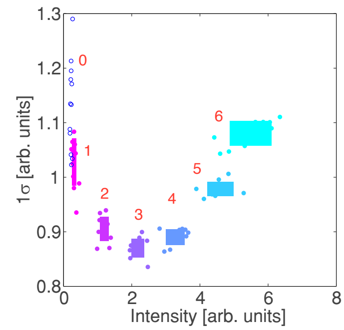

Figure 6: The bunch-by-bunch beam size (1σ) measurement in the 7×12 buckets for an LHC beams in the PS at extraction energy.

It is worth noting that the three clusters of 6 bunches noted with the number 4, 5 and 6 show a different beam σ that depend linearly on the intensity of the bunch (as expected). The signal of the cluster 1, 2, and 3 is too noisy (the PM voltage was optimized for the higher intensity of clusters 4, 5) and can be compared to the cluster 0 corresponding to the abort gap (no signal, pure noise). The transition between the σ of the clusters 4 and 5 is clearly visible. From that observation we can conclude that, for a correct setting of the PM, the cross-talk between adjacent bunches introduced by the signal chain is negligible.

CONCLUSIONS

In this work, we presented a beam-based method to verify the linearity of the horizontal wire scanner calibration with respect to the beam dispersive orbit. The maximum error on the slope of the calibration curve is ≈10% for radial displacement from -20 to +25 mm. This impacts the instrument accuracy. In the worst case (e.g., pencil beam with $\sigma \approx 1$ mm), the relative accuracy error of the measured beam σ can go up to 10% for measurements at different radial positions. To conclude about the absolute accuracy of the WS for a given radial position, further investigations are needed on the PU calibrations and on the model of the machine dispersion. A general deconvolution algorithm to compute the beam betatronic distribution was presented. It is based on transforming the convolution equation in a matrix multiplication and solving it using a standard regularization algorithm. In addition, the results of the first PS bunch-by-bunch emittance measurements, based on numerical gating, were reported. In the tested beam conditions, the cross-talk between adjacent bunches at 25 ns spacing is marginal.

ACKNOWLEDGMENT

The authors are pleased to acknowledge the CERN Emittance working group, the PS operation team, G. Arduini, J. Bellman, S. Hancock, J. F. Herranz Alvarez, E. Métral, G. Métral, Y. Papaphilippou, A. Oeftiger, R. Scrivens and R. Steerenberg for the support and the fruitful discussions.

ISBN 978-3-95450-147-2

REFERENCES

[1] R. Garoby et al., Plans for the Upgrade of the LHC Injectors, IPAC2011,San Sebastian, Spain, WEPS017, pp. 2517–2519, 4-9 September 2011.

[2] G. Rumolo et al., Expected Performance in the Injectors at 25 ns without and with Linac4, Review of LHC and Injector Upgrade Plans Workshop, Archamps, France, 29-31 October 2013.

[3] G. Sterbini et al., Beam-base measurement of the CPS Wire Scanner Precision and Accuracy, IPAC2014, Dresden, Germany, pp. 3674–3676, 15-20 June 2014.

[4] Ch. Steinbach, Emittance measurements with the CERN PS wire scanner, Workshop on Emittance in Circular Accelerators, Tsukuba, Japan, 21-26 November 1994.

[5] F. Roncarolo, Accuracy of the Transverse Emittance Measurements of the CERN Large Hadron Collider, PhD Thesis, EPFL, 2005, Lausanne.

[6] M. Benedikt et al., Injection Matching Studies Using Turn By Turn Beam Profile Measurements on the CERN PS, DIPAC2001, Grenoble, France, 13-15 May 2001.

[7] E. Bravin et al., A new TV beam observation system for CERN, DIPAC2005, Lyon, France, 6-8 June 2015.

[8] R. Veness et al., Design of High-Precision Fast Wire Scanner for the SPS At CERN, IBIC2012, Tsukuba, Japan, 1-4 October 2012.

[9] D. Bodart, Development of an Ionization Profile Monitor Based on a Pixel Detector for the CERN Proton Synchrotron, IBIC2015, Melbourne, Australia, 13-17 September 2015.

[10] P.W. Krempl, The Abel-type integral transformation with the kernel $(t^2 - x^2)^{-1/2}$ and its application to density distributions of particle beams, CERN MPS/Int. BR/74-1, CERN, Geneva, Switzerland, 1974.

[11] S. Hancock, A simple algorithm for longitudinal phase space tomography, PS/RF/Note 97-06, 1997, CERN, Geneva, Switzerland.

[12] A. Oeftiger et al.,“Flat Bunches with a Hollow Distribution for Space Charge Mitigation”, Busan, Korea, 8-13 May 2016, this conference

[13] A. Oeftiger et S. Hancock, “Hollow bunches”, presentation in the Machine Studies Working Group, CERN, Geneva, Switzerland, 4 March 2016.

[14] I. Selesnick, Least Squares with Examples in Signal Processing, lectures of New York University Tandon School of Engineering, 7 March 2013.